Adaptive Multi-modal Sensors

Kyle I. Harrington[1] and Hava T. Siegelmann[2]

[1] School of Cognitive Science, Hampshire College, Amherst, MA 01002 USA
kyle@kephale.com
[2] Department of Computer Science, University of Massachusetts, Amherst, MA 01003 USA

Abstract. Compressing real-time input through bandwidth constrained connections has been studied within robotics, wireless sensor networks, and image processing. When there are bandwidth constraints on real-time input the amount of information to be transferred will always be greater than the amount that can be transferred per unit of time. We propose a system that utilizes a local diffusion process and a reinforcement learning-based memory system to establish a real-time prediction of an entire input space based upon partial observation. The proposed system is optimized for dealing with multi-dimension input spaces, and maintains the ability to react to rare events. Results show the relation of loss to quality and suggest that at higher resolutions gains in quality are possible.

1 Introduction

Sensor systems are often required to transfer spatially related data across bandwidth constrained connections. This data can come from many forms: visual, auditory, electrical, etc. [1,2,3,6,8,9,19,21]. We propose a system that compensates for these constraints by accessing a subset of the available input and performs a real-time spatio-temporal extrapolation for the values of the unknown input. The result of this extrapolation is an expectation of the input space. Once an expectation of the input space is established behaviors can be performed, such as reacting, planning, and learning [12,20]. The result of the system is a smaller input size causing a faster update rate, this increases the potential for reactivity, the relevancy of plans, and pertinence of knowledge. The system described in section 2 performs this recreation.

Embodied intelligent systems have sensorimotor loops. These loops allow such systems to observe the environments with which they may interact. Intelligent systems can then learn to exploit sensorimotor relationships within the environment, for example causal relationships. The work of Lungarella and Sporns provides a foundation for understanding how to learn and exploit such relationships [7]. The authors suggest an inherent link between a system's physical representation and information flow within the system. However, in order to exploit such relationships the system must have an internal representation of its physical state.

M. Lungarella et al. (Eds.): 50 Years of AI, Festschrift, LNAI 4850, pp. 164–173, 2007.

An internal representation of physical state and innate knowledge of the sensor and motor systems is not always given; however, they can be learned. Olsson *et al.* describe a system which learns a model of its sensorimotor system with no *a priori* knowledge [10]. The system initially performs exploratory actions to develop a map of the relationships between the sensor and motor systems. An entropy based metric is used for measuring the informational distance between sensors. The system which is described in this paper follows an alternative approach of strictly utilizing spatial and temporal relationships between sensors.

Related work in robotics, wireless sensor networks, and image processing approach the bandwidth constraint problem at different levels. Rixner *et al.* use a bandwidth hierarchy specific to media applications [13]. Webb developed a new set of communications primitives for parallel robotics image processing [19]. Hull, Jamieson, and Balakrishnan used a rule-based approach for real-time bandwidth allocation [4]. The proposed system uses temporal and spatial information to allocate bandwidth in real-time.

A similar approach was investigated by Schneider *et al.* in a power grid control application in which distributed value functions were used. Their system allows nodes to learn a value function which estimates future rewards at every node in the system [14]. In the context of the proposed system this means that each sensor stores an estimate of all activity in the system. The most prominent difference is that diffusion is used as the method for distributing this estimate along the sensor grid.

2 System

The system consists of a lattice of locations where sensors can reside. Each and every sensor is capable of accessing multiple types of input at its location. Examples of these types of input are red, green, and blue sensing modes Sensor activation ranges from $[0, 1]$ for each mode. 0 means that there is no activity in the given mode, and 1 means the mode is maximally active. Each type of input is referred to as a sensing mode. By adaptively selecting each sensor's active sensing modes based upon a set of sensor memory chemicals it is possible to reduce the number of sensors necessary to adequately sense the environment, as well as the reduce the amount of bandwidth used by sensors. These reductions are the result of an iterative chemical diffusion process. These components are further described in the following subsections.

2.1 Sensors

The sensors are homogeneous, in that each sensor is capable of sensing the same number of modes as the others. In order to replicate the observed environment every sensor must observe every mode in the environment, this is equivalent to performing a complete copy of the environment. However, in many cases the environment changes in a temporally related manner. This temporal relation is exploited by sensing fewer than the total available number of modes, and

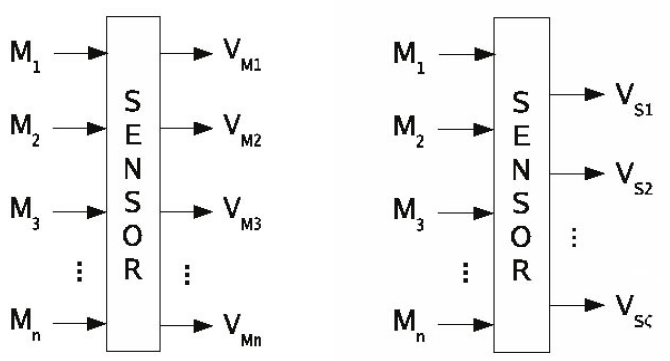

Fig. 1. First, a sensor accessing all n modes at once which requires n observations. Second, a sensor accessing ζ dynamically selected modes which requires ζ observations, where $\zeta < n$.

extrapolating the values of modes based upon learned sensor histories, which we refer to as chemical because they are distributed via diffusion.

2.2 Sensor Chemicals

Sensor activity is stored in chemicals just as value functions are learned by temporal-difference reinforcement learning[15]. For each sensing mode, there are two chemicals that act as sensory memory, C_S, short-term memory and C_L, long-term memory. The parameters γ_S and γ_L are the discount-rate, the rate at which a value fades from memory, and $\gamma_S < \gamma_L$. These chemicals are produced by the rate equations

$$C_S = C_S + \alpha((S_A + \gamma_S C_S) - C_S)$$
$$C_L = C_L + \alpha((S_A + \gamma_L C_L) - C_L)$$

where, S_A is the activation value of the sensor for mode A, and α is the learning rate. In this case *state* refers to the chemical configuration. An example of sensor chemicals within a sensor changing over time can be seen in figure 2. The sensor chemicals also represent short- and long-term activation values. This allows the short-term chemical to be used directly for reconstruction.

In order for the system it must be able to reconstruct an expectation of the environment based upon the current chemical configuration. Reconstruction is a simple local process performed at each sensor for every sensing mode. If the sensor has already observed activity in the given mode, then the activity is already known and that value is used. Otherwise, the value of the short-term chemical is used. This allows the system to automatically maintain expectations of activity in every observable mode.

The diffusion coefficients of the sensor chemicals are numbers in the range of $[0, 1]$. This allows the system to exhibit a continuum of behaviors. When the diffusion coefficient is set to 0 all local history is retained, to 1 all local history is

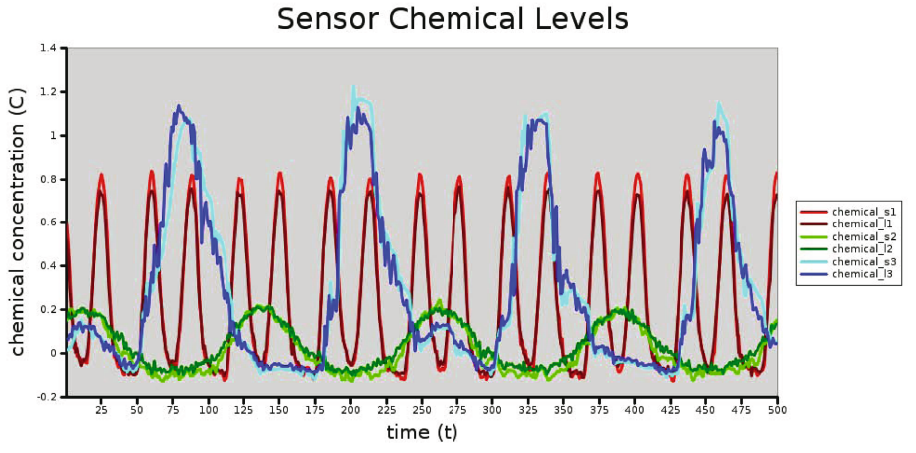

Fig. 2. Sensor chemicals over time for an example sensor. 2 of 3 possible modes were active in this case. The sensor switches its 2 active modes based upon the current concentration of short- and long-term chemicals.

distributed to neighboring sensors causing a global history. The diffusion coefficients allow control to be exercised on the amount of information that is shared amongst neighboring nodes.

2.3 Diffusion

The premise for using diffusion is inspired by Turing's explanation of pattern formation by reaction-diffusion [17]. Two properties appear by diffusion. First, older information can be retained. By diffusing off the edges of the lattice some information is lost. Second, localized diffusion propagates information globally over time, allowing sensors to anticipate unobserved activity. Diffusion occurs according to $C_r^i = C_r^i + D_i \sum_{r \sim r'} (C_{r'}^i - C_r^i)$, where C^i is the amount of sensor chemical i, and D_i is the diffusion coefficient for sensor chemical i. The relation $r \sim r'$ is held for the Von Neumann neighborhood [18] of the target node for diffusion along the lattice, and the relation $r \sim r'$ is from a sensor to the node it occupies for diffusion into the sensor.

2.4 Sensor Mode Selection

A variable $\zeta \in [0, m]$, where m is the total number of modes, controls the number of active modes in each sensor. ζ modes are selected incrementally using ϵ-greedy based on the greatest difference between C_S and C_L for each mode. The ϵ-greedy selection process has two results, the greedy result where the selected mode $max(C_S - C_L)$, or the random result where a random mode is selected. Greedy is always selected, unless $p < \epsilon$, where p is the probability of selecting a random mode [16]. As is mentioned with respect to sensing rare events, the value of ϵ controls the minimum frequency at which events can be detected.

2.5 Sensing Rare Events

The sensing of rare events is heavily reliant on the use of ϵ-greedy selection for modes. By increasing the value of ϵ towards 1 it is possible to detect more rare events by the random selection; however, it decreases the performance on sensing the overall environment. In most cases it is more beneficial to, instead of or in conjunction to increasing the value of ϵ, to increase the number of active modes. This is because ϵ-greedy selection is applied for each mode to be sensed during a given update.

2.6 Observed Environment

The specifications for an environment are minimal. The environment must have a function that returns the value for a region defined by a point and a radius, shown in figure 3. In our case the radius is a Von Neumann neighborhood radius and the value for the region is the sum of activity at each point within that region, Fig. 3 illustrates this. The environment can consist of multiple modalities to be sensed, in this case a function is necessary for each mode. It is also possible for the observed environment to be dynamic with respect to time. The dynamics of the environment should be spatially and temporally related.

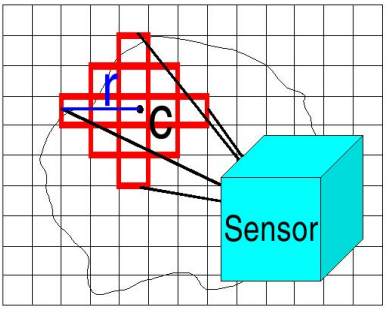

Fig. 3. Sensor with center, c, and radius, r=2. This sensor would return the sum of the values of each highlighted cell.

3 Experiments

3.1 Experiment I: Rare Events Are Detected

The system's ability to detect rare events was evaluated in an environment with a blue background and one small red circle, which moved across the environment infrequently from some same edge 4 times over 1000 iterations. The area of the red circle was 7% of the entire environment. A prevalent tactic for compression is spatial generalization; however, when generalizing based on the spatial relationships of sensory information it is frequent that small rare events may

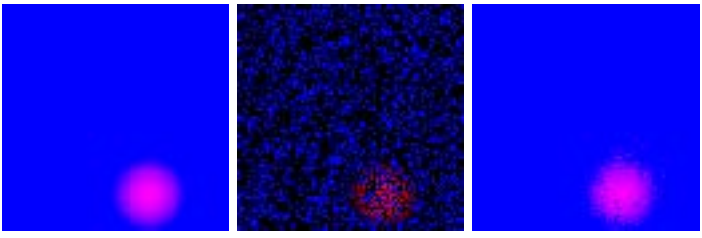

Fig. 4. Snapshot of experiment I, a blue environment with red circle that moves into the environment periodically. First is the original image. Second are the observations colored for respective their modes, black sensors are observing modes for which there is no activity. Third is the chemical prediction of original image. The environment and the sensor lattice are 100x100, the red circle is of radius 15. $\zeta = 1$, meaning only one color can be sensed by any given sensor.

be filtered out. The use of the ϵ-greedy method allows for small rare events to be fairly easily detected if the value of epsilon is adjusted according to the size of potential rare events. The system strictly favors more recent sensor memory, regardless of its value. This experiment was designed to test whether the system was still capable of responding to new events even after saturating its memory with a single mode.

For the case of rare events the set of parameters that were of the most interest were a mode compression of $\zeta = 1$ given a blue background and a relatively small mobile red event. This is because this parameter setting allows the system to be saturated with activity from one mode, then a rare event from another mode is presented. The detection of the rare event can then be observed. Results for $\zeta = 1$ for 100x100 environments had an average error less than 2.5%. The quality of this detection is exemplified in Fig. 5, which illustrates a 100x100 observed environment with no resolution compression, and a mode compression of 1.0.

3.2 Experiment II: Simultaneous Activity Is Observed for All ζ

This experiment was designed to demonstrate the system's ability to handle simultaneous activity. For this experiments there were 3 modes which were represented by the colors, red, green, and blue. All instances were evaluated for 1000 iterations. The experiment utilizes three trajectories, each represented by a different colored circle. The trajectories are as follows: red, a half-circle from top-left to bottom-left, green, a circle rotating around the environment, and blue, a horizontal hourglass across the environment. The trajectories were selected such that each combination of overlapping circles occurred multiple times. This is to ensure that even with small values of ζ all modes are still sensed. This environment was evaluated in three cases, A, a 10x10 observable environment and 10x10 sensor lattice, B, a 100x100 observable environment and 10x10 sensor lattice, and C, a 100x100 observable environment and 100x100 sensor lattice.

Our results show the utility of this system with variety of dimensions of the sensor grid and environment with respect to simultaneous activity. We evolved a

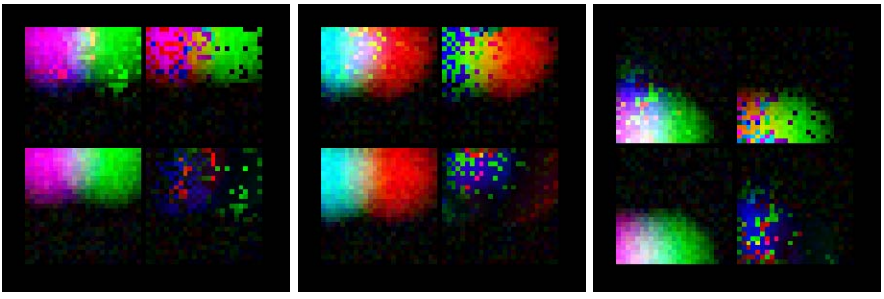

Fig. 5. Image of the system demonstrating the ability to represent 3 modes with 2 active modes. Three circles, one for each mode, follow unique trajectories with multiple intersections. Images of 3 of these intersections are shown, each of which has the following 4 displays Top left, sensors' prediction of the environment. Top right, activity recorded by sensors. Bottom left, original image. Bottom right, the absolute value of difference between the original and predicted image.

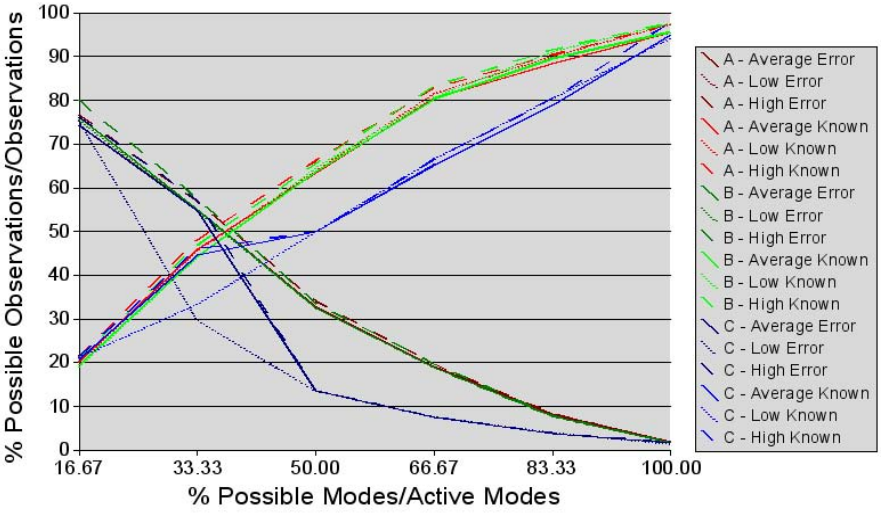

Fig. 6. Results for the three cases in experiment II, A, a 10x10 observable environment and 10x10 sensor lattice, B, a 100x100 observable environment and 10x10 sensor lattice, and C, a 100x100 observable environment and 100x100 sensor lattice. The relationship between the number of active modes and prediction accuracy is shown. For cases A and B the percent error is approximately equal to the amount of the environment that is not observed. For case C the percent error is less than the amount of the environment that is not observed.

population of 50 parameter settings for $1,000$ different parameter settings. Fig.6 illustrates the effect of mode compression, $\frac{\zeta}{m}$ where m is the number of modes, on the quality of the final product. We define this quality in terms of prediction error, which is simply defined as the difference between the original image and

the prediction summed over all modes for all sensors. Cases A and B show the system producing results of approximately equal quality to percentage of the environment that is known. Both of these cases consisted of low resolution grids, yet the system still maintained an output that was at least consistent with the amount of compression, if not actually providing enough inference to reduce the error beyond minimal expectation. In both cases the amount of error and the amount of compression sum up to approximately 100%. This means the amount of error is equivalent to the amount of the environment that the system did not observe. The similarity between the cases A and B suggest that the size of the sensor grid limits the quality of the compression. Case C illustrates the difference between compression and error with an image of higher resolution. The compression and error sum to significantly less than 100%.

4 Conclusions

It is important that the results with low resolutions show the compression to maintain a total quality that does not decrease beyond that of unprocessed input with an equivalent bandwidth constraint. This observed quality threshold is suggestive when considered with the results in Fig. 8. By increasing the resolution of the image it possible for the quality to increase above the quality of uncompressed data through an equivalently small bottleneck. This suggests that it is possible for high resolution images to maintain smaller storage and/or network transfer footprints. These benefits are similar to those Kansal et al. obtained by using motion control [5].

We have presented a system which allows real-time input to be scaled through a bandwidth constraint while maintaining a level of quality appropriate to the amount of compression used. The system does not require any overhead bandwidth, instead selects which values from the environment are transferred. Values are recorded as sensor chemicals which are diffused across the sensor grid. When used at higher resolutions, some values of ζ allowed for quality surpassing 100%. Our results suggest that this system is useful for compressing some types of real-time input through bandwidth constraints.

5 Future Work

Future work will investigate an implementation of the previously described system in a 3-dimensional environment. Additionally, discretization of sensor input will be used to further reduce bandwidth usage [11]. Embodied implementations of this system should investigate sensorimotor regularities induced by the addition of a motor system for further optimization [7].

Acknowledgements

We acknowledge funding from NSF grant ECS-0501432.

References

1. Babilonia, F., Mattiab, D., Babilonia, C., Astolfib, L., Salinarie, S., Basiliscoa, A., Rossinic, P.M., Marcianib, M.G., Cincotti, F.: Multimodal integration of EEG, MEG, and fMRI data for the solution of the neuroimage puzzle. Magnetic Resonance Imaging 22, 1471–1476 (2004)
2. Gottesfeld Brown, L.M.: Registration of Multimodal Medical Images - Exploiting Sensor Relationships. PhD thesis, Columbia University (1996)
3. DuFaux, F., Moscheni, F.: Motion estimation techniques for digital TV: A review and a new contribution. Proceedings of IEEE 83(6), 858–876 (1995)
4. Hull, B., Jamieson, K., Balakrishnan, H.: Bandwidth management in wireless sensor networks. Technical report, Massachusetts Institute of Technology (2003)
5. Kansal, A., Kaiser, W., Pottie, G., Srivastava, M., Sukhatme, G.S.: Virtual high-resolution for sensor networks. In: ACM SenSys, ACM Press, New York (2006)
6. Kulkarni, P., Ganesan, D., Shenoy, P., Lu, Q.: Senseye: a multi-tier camera sensor network. In: MULTIMEDIA 2005. Proceedings of the 13th annual ACM international conference on Multimedia, New York, NY, USA, pp. 229–238 (2005)
7. Lungarella, M., Sporns, O.: Mapping information flow in sensorimotor networks. PLoS Computational Biology 10, 1301–1312 (2006)
8. Mario, X.H.: Load balanced, energy-aware communications for mars sensor networks. In: IEEE Aerospace Conference Proceedings (2002)
9. Olsson, L., Nehaniv, C.L., Polani, D.: Sensory channel grouping and structure from uninterpreted sensor data. In: Proceedings of NASA/DoD Conference on Evolvable Hardware (2004)
10. Olsson, L., Nehaniv, C.L., Polani, D.: From unknown sensors and actuators to visually guided movement. In: Proceedings of the 4th International Conference on Development and Learning (2005)
11. Olsson, L., Nehaniv, C.L., Polani, D.: Sensor adaptation and development in robots by entropy maximization of sensory data. In: CIRA 2005. Proceedings of IEEE International Symposium on Computational Intelligence in Robotics and Automation (2005)
12. Prati, A., Vezzani, R., Benini, L., Farella, E., Zappi, P.: An integrated multi-modal sensor network for video surveillance. In: VSSN 2005. Proceedings of the third ACM international workshop on Video surveillance & sensor networks, New York, NY, USA, pp. 95–102 (2005)
13. Rixner, S., Dally, W.J., Kapasi, U.J., Khailany, B., Lopez-Lagunas, A., Mattson, P.R., Owens, J.D.: A bandwidth-efficient architecture for media processing. In: International Symposium on Microarchitecture, pp. 3–13 (1998)
14. Schneider, J., Wong, W.-K., Moore, A., Riedmiller, M.: Distributed value functions. In: Proceedings of the 16th International Conference on Machine Learning, pp. 371–378. Morgan Kaufmann, San Francisco, CA (1999)
15. Sutton, R.S.: Learning to predict by the methods of temporal differences. Machine Learning 3, 9 (1988)
16. Sutton, R.S., Barto, A.G.: Reinforcement Learning: An Introduction. MIT Press, Cambridge (1998)
17. Turing, A.M.: The chemical basis of morphogenesis. Philosophical Transactions of the Royal Society of London. Series B, Biological Sciences 237(641), 37–72 (1952)
18. von Neumann, J.: Theory of Self-Reproducing Automata. University of Illinois Press, Urbana, Illinois (1966)

19. Webb, J.A.: Latency and bandwidth considerations in parallel robotics image processing. In: Proceedings of Supercomputing, pp. 230–239 (1993)
20. Weise, T., Geihs, K.: Genetic programming techniques for sensor networks. In: Proceedings of 5. GI/ITG KuVS Fachgespräch "Drahtlose Sensornetze", pp. 21–25 (2006)
21. Zhao, Y., Garden Richardson, I.E.: Computational complexity management of motion estimation in video encoders. In: DCC, p. 483. IEEE Computer Society, Los Alamitos (2002)